POLITECNICO DI TORINO
Repository ISTITUZIONALE

A preliminary methodology to assess gust spectra via satellite data

Original
A preliminary methodology to assess gust spectra via satellite data / Carrera, E., Pagani, A., Valente, M., Palaia, G.. - In: ADVANCES IN AIRCRAFT AND SPACECRAFT SCIENCE. - ISSN 2287-5271. - 12:1(2025), pp. 25-43. [10.12989/aas.2025.12.1.025]

Availability:
This version is available at: 11583/3001511 since: 2025-07-09T13:12:58Z

Publisher:
Techno-Press

Published
DOI:10.12989/aas.2025.12.1.025

Terms of use:

This article is made available under terms and conditions as specified in the corresponding bibliographic description in the repository

Publisher copyright

(Article begins on next page)

16 November 2026

Advances in Aircraft and Spacecraft Science, *Vol. 12, No. 1 (2025) 25-43*
https://doi.org/10.12989/aas.2025.12.1.025

A preliminary methodology to assess gust spectra via satellite data

Erasmo Carrera[a], Alfonso Pagani[b], Marianna Valente[c] and Giuseppe Palaia*

Mul2 Group, Department of Mechanical and Aerospace Engineering, Polytechnic of Turin, Corso Duca degli Abruzzi 24, 10129, Turin, Italy

(Received December 3, 2024, Revised February 22, 2025, Accepted February 25, 2025)

Abstract. This paper investigates the power spectral density (PSD) of wind gusts by utilizing data from Low Earth Orbit (LEO) satellites. The wind gust represents one of the most unpredictable phenomena; indeed, its transient nature presents significant challenges in the aircraft design. Aircraft structural components are designed to deal with fatigue loads generated by the turbulent movement of the air, which, due to the ongoing changes of climate, may increase more and more and affect the safety of the aircraft. The effects of gusts on the structural integrity are typically evaluated through power spectral analysis, which provides a realistic representation of the air movement. The potential impact of climate change on gust spectra urges to incorporate recent data, and satellites are a valuable resource for this purpose. The analysis is divided into two parts: the first combines power spectral analysis with LEO satellite data to assess PSD of vertical wind gust based on von Kármán model (PSD_{vk}); the second compares the PSD_{vk} with the PSD assessed via a model, named "agnostic" (PSD_a), which does not rely on a pre-defined equation. The results, focusing on a part of the transatlantic route, show that the proposed approach allows to reveal annual and seasonal fluctuations in gust patterns. The comparison between PSD_{vk} and PSD_a reveals that some differences may occur at high frequencies. These findings highlight the potential of satellite technology to monitor climate change's effects and establish a foundation for further research in this critical area.

Keywords: climate change; gust; LEO satellite; power spectral analysis; power spectral density

1. Introduction

Reliability and safety are an indispensable duo in aeronautics, enabling aircraft to fly while minimising the risk of accidents. Human factors (e.g., situational awareness, errors in procedures) (Kharoufah *et al.* 2018), and structural component failures (Findlay *et al.* 2002) are some of the causes of aircraft accidents. Human factors and structural component failures are also influenced by adverse weather conditions. In fact, extreme weather events (e.g., gusts of high intensity), may increase the amount of human factors errors and generate high loads for the aircraft structural components, potentially affecting passenger safety (Sharman 2016). These aspects are of crucial importance since i) aviation is expanding rapidly (Graver *et al.* 2019), ii) due to climate change

*Corresponding author, Assistant Professor, E-mail: giuseppe.palaia@polito.it
[a]Professor, E-mail: eramo.carrera@polito.it
[b]Professor, E-mail: alfonso.pagani@polito.it
[c]Ph.D. Student, E-mail: marianna.valente@polito.it

Copyright © 2025 Techno-Press, Ltd.
http://www.techno-press.org/?journal=aas&subpage=7 ISSN: 2287-528X (Print), 2287-5271 (Online)

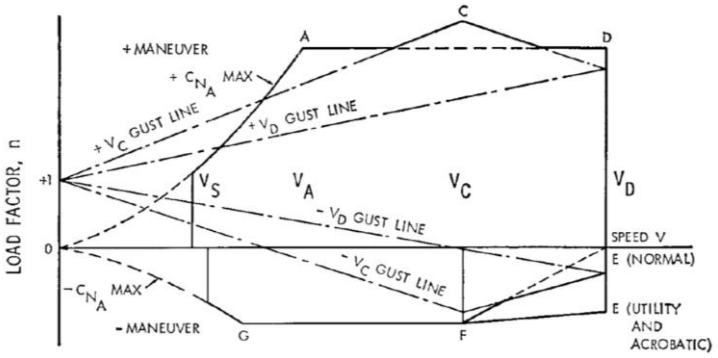

Fig. 1 V-n_z diagram. Image taken from Gudmundsson (2014)

adverse and extreme weather phenomena are becoming more and more frequent (NASA). The increase in the number of flights, which is expected to grow, together with the potential worsening of weather conditions, could lead to an increase in air accidents. In order to ensure high safety standards for aircraft whose entry into service is in the next few years, and which could also like rely on new propulsion technologies such as the hybrid-electric (Abu Salem *et al.* 2023, Figueroa *et al.* 2024) and hydrogen (Bagarello *et al.* 2024), it should be convenient to examine current design procedures and maintenance aspects.

Regarding the design of structural components, the use of the flight envelope is well known in the aviation world. It concerns the combination of manoeuvre and gust loads; in fact, it is given by the envelope of two specific diagrams, the manoeuvre diagram and the gust envelope. Both diagrams depend on the design characteristics of the aircraft (e.g., wing surface), and the gust envelope also depends on the gust intensity, established according to current certification standards. From the flight envelope it is therefore possible to define the combinations of speed V and vertical load factor n_z that must be considered for the structural verification to which the aircraft must be subjected, and for which a specific safety factor must be guaranteed. The shape of the gust diagram therefore depends on both the design parameters of the aircraft and the gust intensity established according to the regulations (Lomax 1996, Gudmundsson 2014) and FAR 25), an example of a V-n_z diagram is shown in Fig. 1.

From the aforementioned description, it is clear that aircraft design concerns not only the aircraft itself but also the surrounding environment, i.e., the air. To ensure adequate safety levels, it is therefore necessary to develop models that are as close as possible to the actual behaviour of the aircraft, atmospheric air movements and their mutual interaction (Yuan *et al.* 2024, Gu *et al.* 2024, Mehmood *et al.* 2023, Jiang *et al.* 2023, Jones *et al.* 2022, Jones *et al.* 2021, Balatti *et al.* 2021, Lee *et al.* 2013, Morelli *et al.* 2012). In this sense, aviation regulations have evolved over time to take this interaction into account more and more accurately (Lomax 1996, Flomenhoft 2012, Hoblit 1988). The earliest regulations considered a gust to be ‘discrete’; this nomenclature derives from the fact that the gust is modelled as an isolated event encountering the aircraft. The shape of the gust has evolved over time from the step shape to the one minus cosine shape; in addition, a reduction factor of n_z has been incorporated to account for both the gust-aircraft interaction and the dependence on aircraft design parameters such as wing loading. The use of a discrete gust is not representative of an actual gust, which is irregular in the time domain, i.e., it has no repeating patterns; therefore, regulations have been evolved identifying a mathematical model which

represents the gust as a continuous non-periodic function. This model, called turbulent gust, defines the gust in the frequency domain and allows for a more accurate and representative model of the actual behaviour of the gust. This type of approach has a twofold purpose, on the one hand to be able to model and characterise gust shapes that cannot be represented by the discrete model (e.g., gusts that have a very short and intense temporal or spatial duration) and on the other hand to use frequency domain analysis techniques to characterise the gust (Hoblit 1988, Hajjem *et al.* 2023, Press *et al.* 1954). To use this type of approach, the temporal profile of the gust is idealized as a stationary Gaussian random process Hoblit (1988). The use of these models is currently used in various aspects of aircraft design, in evaluating the dynamic response of the aircraft to gusts, in assessing the loads acting on the aircraft due to the interaction with turbulent air motions, and in the static and fatigue sizing of structural components that are subjected to these loads. In this regard, load-alleviation techniques are currently being studied to reduce the aerodynamic loads acting on the aircraft structure, especially under challenging conditions like gusts, turbulence, or maneuvering (Regan *et al.* 2012, Toffol *et al.* 2023, He *et al.* 2021, De Gaspari *et al.* 2016, He *et al.* 2023, Handojo 2022). These loads can significantly impact aircraft structural mass; to mitigate this detrimental effect, load alleviation systems aim to optimize aircraft response in real-time by adjusting control surfaces (such as ailerons, flaps, and spoilers) or through more advanced control systems like active load alleviation. Comprehensive reviews regarding the gust modelling and the effect of climate change, the gust-aircraft interaction and the loads generated due to their mutual interaction are reported in (Wu *et al.* 2019, Storer *et al.* 2019b).

As stated before, gust generates a random load which affects aircraft structure that has to be designed to deal with the phenomenon named fatigue. Fatigue refers to the progressive and localized structural damage that occurs when a material is subjected to cyclic loading (Tavares *et al.* 2017, Filippi *et al.* 2023). Wind gusts contribute to this cyclic loading by introducing variable stress patterns, indeed repeated exposure to gust-induced loads can initiate and propagate cracks in structural components, ultimately leading to material fatigue. This growth of cracks is addressed during the maintenance phase of the aircraft using a damage tolerance approach, which relies on historical data collected and modelled based on transatlantic route gusts (Wu *et al.* 2019, Jones 2014) In the 1930s, detecting and modeling gusts required organizing special flight campaigns, selecting specific routes, and flying a fleet of aircraft to collect the necessary data (Wu *et al.* (2019)). This process often involved substantial financial outlays and extended timeframes, with data typically limited to specific geographic areas. The influence of climate change on gust patterns necessitates implementing more comprehensive and adaptive strategies for understanding and mitigating their effects on aircraft design and operation. Satellites with various sensors and instruments offer a comprehensive dataset that could revolutionize the detection of hazard event such as clear air turbulence, wind shear hurricanes and thunderstorms. Advanced predictive models that employ real-time observations of temperature, humidity and wind velocity can predict turbulence-prone zones (Storer *et al.* 2019a, Lee *et al.* 2023, Kaplan *et al.* 2006). Real-time monitoring through satellites, such as RainCube and TEMPEST-D, significantly enhances aviation hazard detection (Radhakrishnan *et al.* 2022). These technologies, exemplified by METEOSAT, a series of seven meteorological geostationary satellites operated by EUMETSAT, play a crucial role in predicting convective initiation and identifying clear air turbulence (Nerushev *et al.* 2022). In this context, this article aims at exploiting satellite technology to detect and analyze wind gust data, and leveraging on power spectral analysis techniques to assess wind gust power spectral density. This work is organized as follows: Section 2 delves into the possibilities of utilizing satellite data to detect variations in wind gusts; Section 3 elucidates the methodology employed to

Fig. 2 Satellite projection onto the Earth's surface over a 24-hour period. Image adapted from (ESA)

analyze the satellite data; Section 4 presents findings, specifically examining gusts across different periods of the year, and in different years; Section 5 discusses the limitations of the approach; and finally, Section 6 offers insightful reflections and conclusions.

2. Satellite technology to forecast gust

The rise of satellite technologies has revolutionized the approach to wind gust detection. The ability to access a vast quantity of data relatively quickly and achieve near-global coverage, primarily through low-earth orbit (LEO) satellites, is a significant advantage. This technology also allows for data collection at different altitudes with a single measurement, a capability that was previously unattainable. Moreover, satellites can now carry multiple payloads, enabling the collection of diverse data during a single observation period. These missions extend beyond climate monitoring, showcasing the versatility of satellite technology. Furthermore, the rapid data exchange between satellites and ground stations facilitates real-time monitoring of weather conditions (Crisp *et al.* 2020, Wangì *et al.* 2023). This article showcases the potential of LEO satellite systems, using data from Aeolus satellites, in estimating wind power spectral density.

2.1 Aeolus data

The European Space Agency's Earth Explorer, Aeolus, commenced its mission on August 22, 2018, marking a significant milestone in satellite-based observation. This satellite provides global insights into wind profiles from the Earth's surface to an altitude of 30 km. Aeolus employs the active Doppler Wind Lidars (DWL) method, which enables precise wind speed and direction measurements. The DWL provides indispensable data on wind profiles, offering valuable details on cloud top heights and the vertical distribution of thin clouds and aerosols (Reitebuch *et al.* 2009, Witschas *et al.* 2020). Aeolus orbits at an altitude of 320 km along a nearly polar trajectory, affording nearly global coverage, albeit not continuous monitoring of every region. Satellites in LEO, orbiting at that altitude, travel at a fixed velocity of approximately 8 km/s, completing one full orbit around the Earth in approximately 90 minutes. Due to the Earth's rotation, during the time it takes for the satellite to complete one orbit, the planet will have shifted by approximately 23°. Consequently, over 24 hours—the time it takes for the Earth to complete one full rotation—the satellite will have completed around 16 orbits, ensuring nearly global coverage. Therefore, as depicted in Fig. 2, the continuous shift in position prevents Aeolus from providing continuous

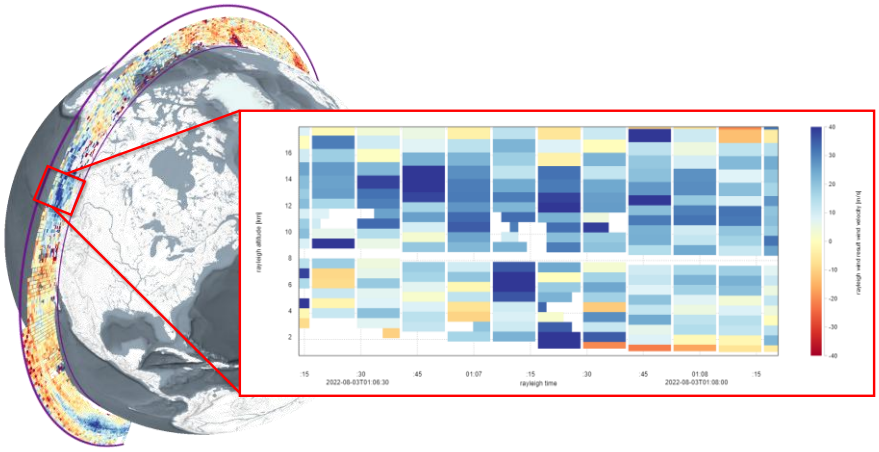

Fig. 3 Representation of the vertical wind gust collected by the satellite at various altitudes along its orbit. Each measurement interval has a height of 1 km, and a width of about 11 s. Image adapted from (ESA)

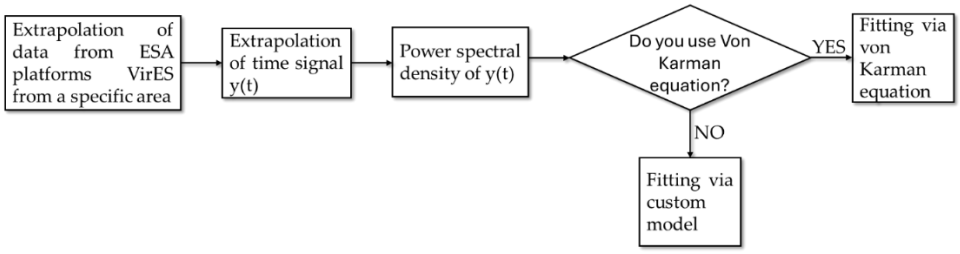

Fig. 4 Workflow adopted in the proposed methodology

coverage over a fixed location, such as the transatlantic route.

As said before, satellite technology enables data acquisition at various altitudes, assessing wind gust variation with altitude and specifying wing direction. As an example, Fig. 3 represents the data about vertical wing gust extracted from Aeolus data on a specific area on USA, and varying altitude from 0 to 17 km. Aeolus conducts measurements every about 11 seconds and scans a range of 30 km with 1 km intervals, as depicted in the graph in Fig. 3. The vast amount of data available and the ability to analyze data at any altitude and geographic location offer numerous opportunities for leveraging these datasets. Although the Aeolus mission spanned only four years, from 2019 to 2022, limiting the examination of gust evolution over time, these data represent a fundamental starting point. Analyzing these datasets has the potential to impact aircraft structural integrity and performance significantly. Indeed, these datasets can be instrumental in deriving aircraft load diagrams and guiding regulatory updates. Additionally, their global coverage, including previously inaccessible routes and altitudes, allows for optimizing aircraft mission trajectories to mitigate the detrimental effects of gusts on performance and support predictive maintenance strategies.

3. Methodology

This section outlines the methodology used to analyze the Aeolus data; specifically, the

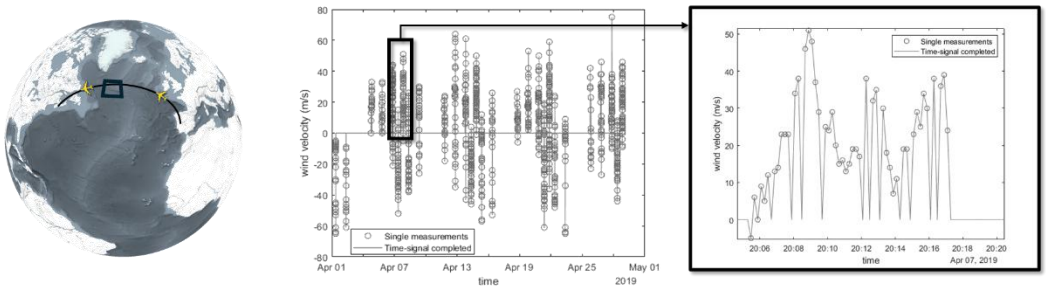

Fig. 5 Data extracted (right image) from ESA platforms VirES in an area (rectangle of left image) of the transatlantic flight route

methodology follows the workflow depicted in Fig. 4. To initialize the procedure, the user has to select a specific area and time horizon in order to extract data from the ESA platform VirES; then the data can be extracted and managed via software such as MATLAB or Python. Finally, the power spectral analyses techniques are employed to assess the power spectral density of the wind gust signal.

The satellite data available on the online ESA platforms VirES were downloaded and analyzed using MATLAB. The VirES platform enables users to select data, define areas of interest, and apply filters to clean the dataset (e.g., by selecting wind direction and altitude). The satellite operates in LEO, so once the area is selected, as the rectangle depicted in Fig. 1-left, wind direction and altitude of that specific area have to be selected. It is worth noting that, as explained in the previous section, the satellite observes the entire earth surface and continuous time observation of the selected area is not possible. The satellite only passes over the selected area twice a day, so the data are available only for a short amount of time. In case the data are not available, the signal is imposed equal to zero (zero padding), as reported in the example of Fig. *5*.

A Discrete Fourier Transform (DFT) technique was applied to the time domain signal to comprehensively analyze its frequency content. This mathematical technique allows to assess its main frequency components, which are calculated according to Eq. (1).

$$X_k = \sum_{n=0}^{N-1} x[n] e^{-i2\pi \frac{k}{N} n} \tag{1}$$

$x[n]$ represents the value of the *n-th* component of the signal $x(t)$ in the time domain evaluated at the time nT, where T is the sample time of the signal, N denotes the total number of samples of the signal (or the length of the signal). The term $e^{-i2\pi \frac{k}{N} n}$ corresponds to a complex sinusoid at frequency $f_k = k/N$, $k \in [0, N-1]$, and X_k represents the associated complex number of the signal in the frequency domain. Eq. (1) gives information about signal's magnitude and phase spectrum in the frequency domain. Specifically, the amplitude spectrum provides information about the intensity of different frequency components in a signal, so allow us to assess how much of each frequency component is contained in the time domain signal. The phase spectrum provides information about the timing and alignment of the frequency components, indicating how the sinusoidal components are shifted in time with respect to the sinusoidal signal which has the same frequency and null phase. Amplitude and phase are relevant for the signal analysis; in particular, the amplitude spectrum gives us an idea about the energy content of each signal component. This

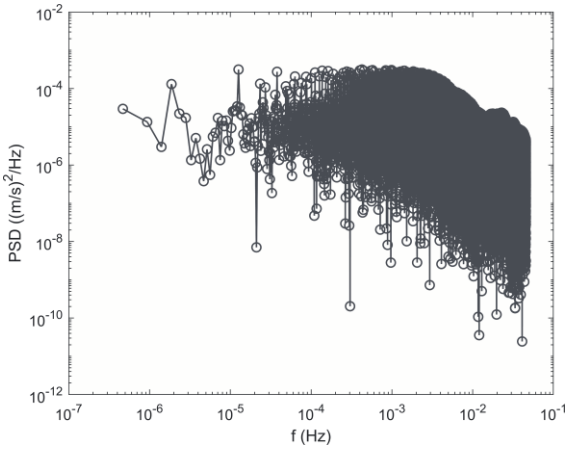

Fig. 6 PSD of vertical wind velocity signal

aspect is well represented by the power spectral density (*PSD*) which is a measure of a signal's power content versus frequency. It shows how the power of a signal is distributed across different frequencies, providing insights into the signal's frequency components. While the amplitude and phase spectra provide detailed information about the individual frequency components, the *PSD* focuses on the power distribution and gives information about the frequencies which contain the highest energy content of the signal. The *PSD* is related to the amplitude of the signal in the frequency domain and is proportional to the square of the amplitude of the signal's Fourier Transform whereas the phase spectrum does not directly influence the *PSD*. The *PSD* has been evaluated using the Eq. (2)

$$PSD(f_k) = \frac{1}{N}|X_k|^2 \tag{2}$$

The result of the application of the power spectral analysis technique is reported in Fig. 6, and show that the signal noise is relevant. In order to assess the actual shape of the *PSD*, Two different methodologies have been chosen to fit the data: the first one which is based on the von Kármán equation, described in Section 0, and the second one, based on an "agnostic" approach, which does not rely on a specific pre-defined equation as explained in Section 0.

3.1 Von Kármán based approach

One of the classical mathematical models to represent the vertical wind gust *PSD* is the von Kármán model (Hoblit 1988), reported in Eq. (3).

$$PSD_{vk}(f) = \frac{\sigma^2 L}{\pi V} \frac{1 + \frac{8}{3}\left(1.339 \times \frac{2\pi L}{V} f\right)^2}{\left[1 + \left(1.339 \times \frac{2\pi L}{V} f\right)^2\right]^{11/6}} \tag{3}$$

where σ represents the root mean square of the wind vertical speed, L stands for the scale of turbulence and V is the true air speed. The von Kármán model is calibrated using two key

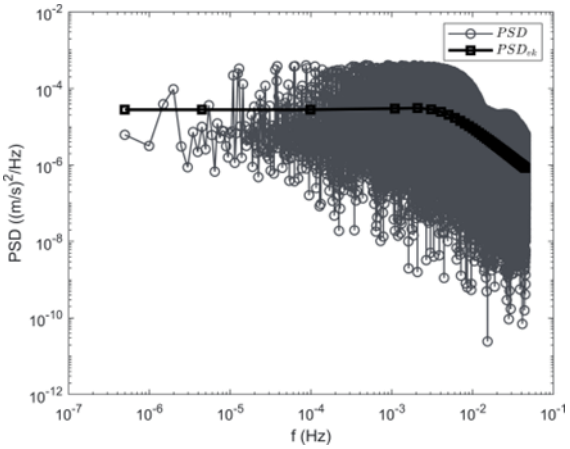

Fig. 7 *PSD* and PSD_{vk} of vertical wind velocity signal

parameters: L and σ. The parameter L represents the frequency at which the slope of Eq. (3) increases and indicates how gust properties vary in space, it is influenced by factors such as altitude, the parameter σ represents the turbulence intensity, which is affected by average wind speed and altitude (Hajjem *et al.* 2023). The parameters L and σ are calculated via a nonlinear least mean square problem in order to find the *PSD* curve which best fits data extracted from the ESA platform VirES. An example of this approach is illustrated in Fig. 7 which shows *PSD* and the PSD_{vk} of vertical wind velocity signal observed in September 2019. The area of observation spanned from 50 to 55 North latitude and from 33 to 43 West longitude and the altitude selected ranged from 9900 to 10900 m. The R^2 of PSD_{vk} is equal to 0.11.

3.2 The "agnostic" approach

The approach described in Section 3.1 is based on the Von Kármán equation which is extensively used in current literature. The Von Kármán equation has been formulated in the first half of the 19th century by using actual data of gust measurements related to that period. Even though the approach is currently adopted also in the aeronautical industry to size structural aircraft components, it is worth noting that due to current changes in the climate behaviour hazard phenomena are more common than in the past (Storer *et al.* 2019b), so a different approach could be adopted in order to capture gust phenomena which in the first half of the 19th century might occur sporadically. To do so, the approach proposed in this section, which has been named "agnostic" since it does not depend on a specific pre-defined equation, is intended to find the best-fit curve of the satellite data without the use of a specific pre-defined equation. As first step a polygonal chain is identified, then an optimization procedure is carried out in order to assess the best-fit curve. The polygonal chain is identified through the following key steps:

1. a set of n points, equally spaced on a logarithmic frequency scale are defined;
2. for each point is calculated a specific frequency f_n and a corresponding value on y-axis y_n is assigned;
3. the polygonal chain is defined by the union of n-1 segments that connect the n points, each segment connects two consecutive points.

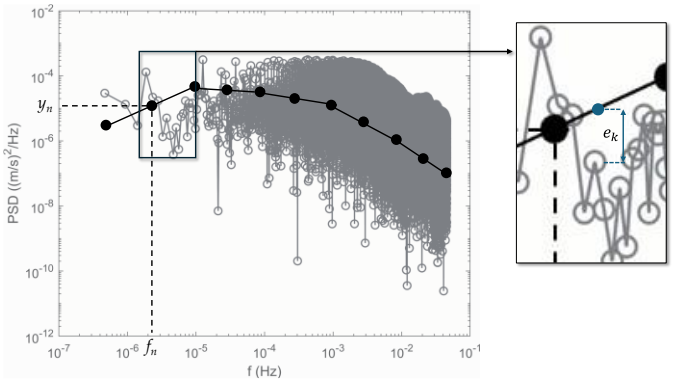

Fig. 8 An example of polygonal chain with n=11

The error e_k between the polygonal chain and the *PSD* is defined according to Eq. (7), where y_k represents the value of the polygonal chain at the *k-th* frequency f_k. An example of the polygonal chain in case of n=11 is depicted in Fig. 8.

$$e_k = y_k - PSD(f_k) \tag{7}$$

Once the polygonal chain is defined, an optimization problem is carried out according to Eq. (8)

$$\begin{cases} min \dfrac{\sum_{k=0}^{N-1} e_k^2(y_n)}{\sum_{k=0}^{N-1}\left(PSD(f_k) - \frac{1}{N}\sum_{j=0}^{N-1} PSD\left(f_j\right)\right)} \\ y_{min} \le y_n \le y_{max} \end{cases} \tag{8}$$

The objective function selected for the optimization problem is the complement of R^2 to one. The design variables are the y coordinates y_n of the n points, which belongs to the polygonal chain, whose upper bound y_{max} and lower bound y_{min} are equal to $10^{-2}\ (m/s)^2/H_z$ and $10^{-12}\ (m/s)^2/H_z$, respectively. The optimization problem employs gradient-based algorithms combined with a multi-start approach to find a solution close to the global minimum. It is worth noting that optimization problem allows to find a polygonal chain which best fits the data; therefore, it allows to find the best-fit curve of the *PSD*. The shape of this curve depends on the number of points n, and this aspect is discussed in Section 0.

4. Results

This section presents the results obtained through the methodology described in Section 0. Satellite data were employed to investigate several observation windows and conduct comparative analyses. Specifically, the following parametric analyses have been carried out:

- **seasonal variation**: one month is selected for each season within a specific year to observe seasonal changes.
- **annual variation**: to assess annual variations, the same month is examined over four years, from 2019 to 2022.

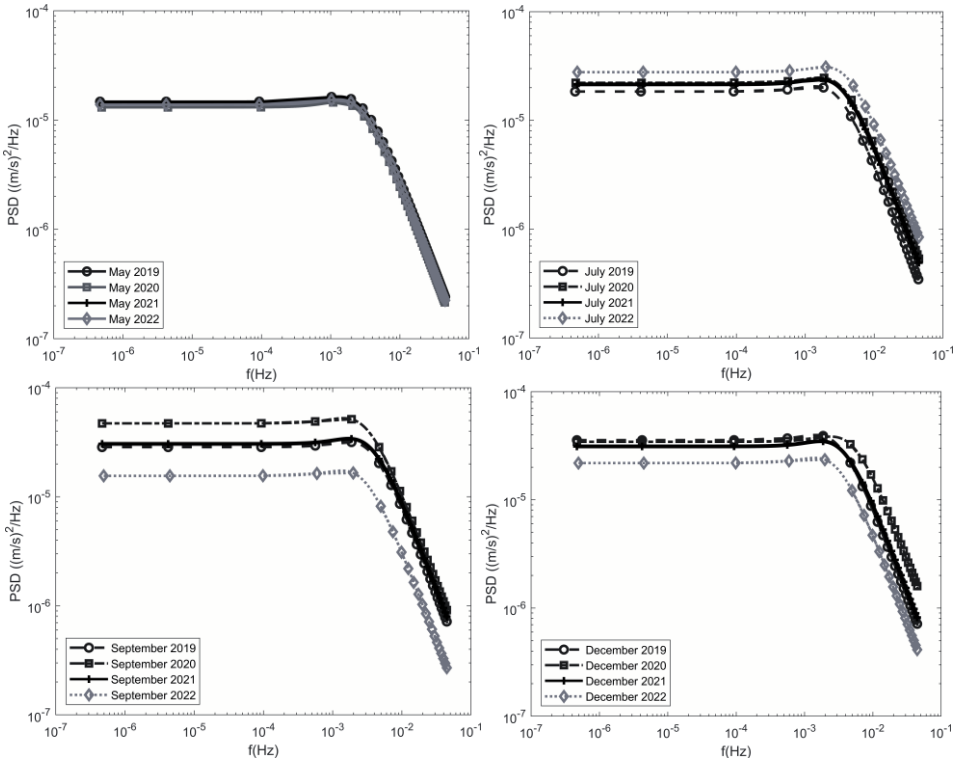

Fig. 9 PSD_{vk} from 2019 to 2022 for different months: May (top-left), July (top-right), September (bottom-left) and December (bottom-right)

The cases examined focus on a segment of the transatlantic route, ranging from 56 to 51 degrees North latitude and from 33 to 43 degrees West longitude (see Fig. 3), and the altitude selected ranged from 9.9 to 10.9 km. These aspects are discussed in Section 0 related to the Von Kármán based approach and Section 0 is related to the "agnostic" approach.

4.1 Analysis of satellite data via von Kármán based approach

This section focuses on the analysis of satellite data via the von Kármán based approach, the outcomes of annual variations are depicted in Fig. 9. The analysis of the data representing the spring season reveals a consistent pattern with no discernible variations over the observed years. In contrast, a variation of the PSD_{vk} in wind gusts is observed from 2019 to 2022 in July, specifically there is a progressive increase in energy at medium-low frequencies. The 2022 curve is the highest one, whereas the 2019 curve is the lowest one. This suggests that, over time, there has been an increase in energy density in the signal, potentially reflecting changes in operational or environmental conditions. This result is not highlighted for September and December, where an opposite trend occurs. A significant month was selected for each season in each year to observe seasonal variations, and the results are presented in Fig. 10. As in the previous analyses, a variety of trends emerge across the years. Across all four years under consideration, the spring season consistently exhibited the lowest gust intensities, followed by summer. Conversely, periods of more intense gusts correspond with the colder months, except in 2022, which showed a notable

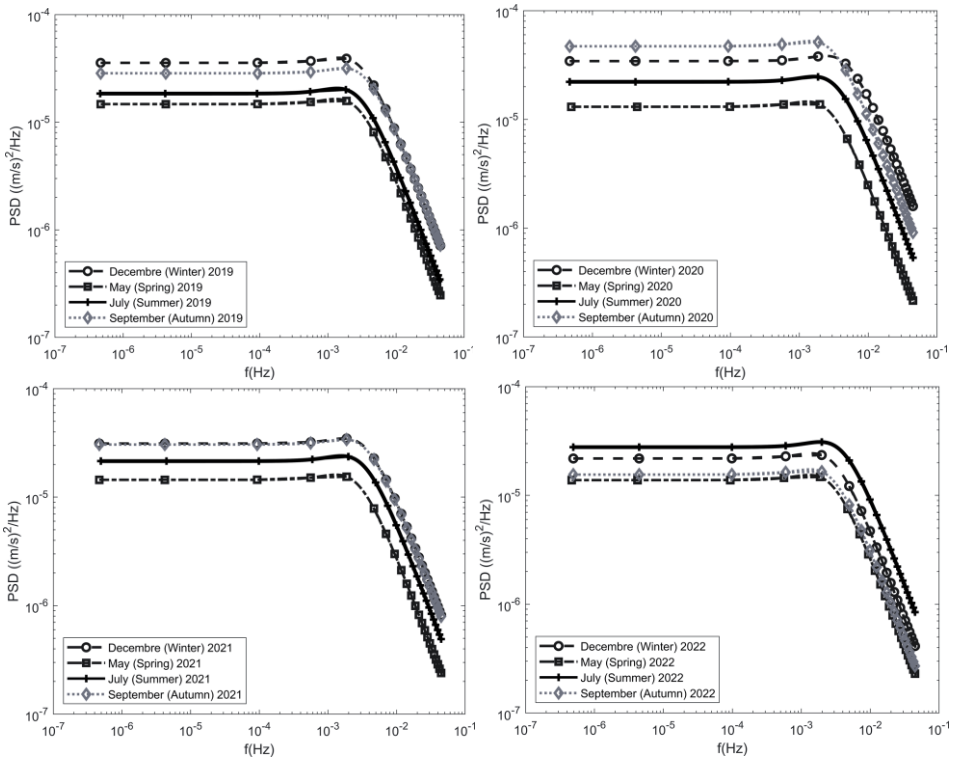

Fig. 10 PSD_{vk} in 2019 (top-left), 2020 (top-right), 2021 (bottom-left) and 2022 (bottom-right) for annual seasons

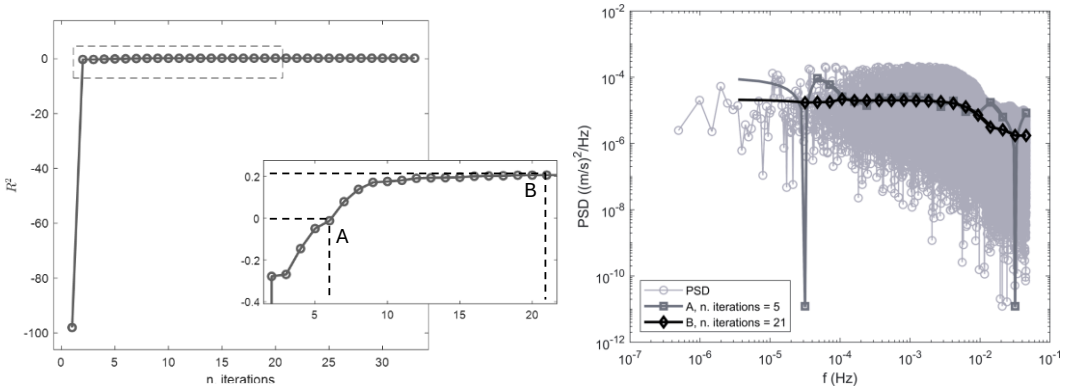

Fig. 11 R^2 vs number of iterations (left) and PSD_a vs frequency (right) of two different cases representative of the beginning of the optimization process (point A) and the end of the optimization process (point B)

increase in gust intensity during summer. The above observations may provide valuable insights from the aeronautical perspective; however, it is essential to note that making predictions based solely on these trends is a not trivial task due to the limited observation period. Nevertheless, they serve as a starting point for subsequent analyses and comparisons with data from other satellites and historical gust records.

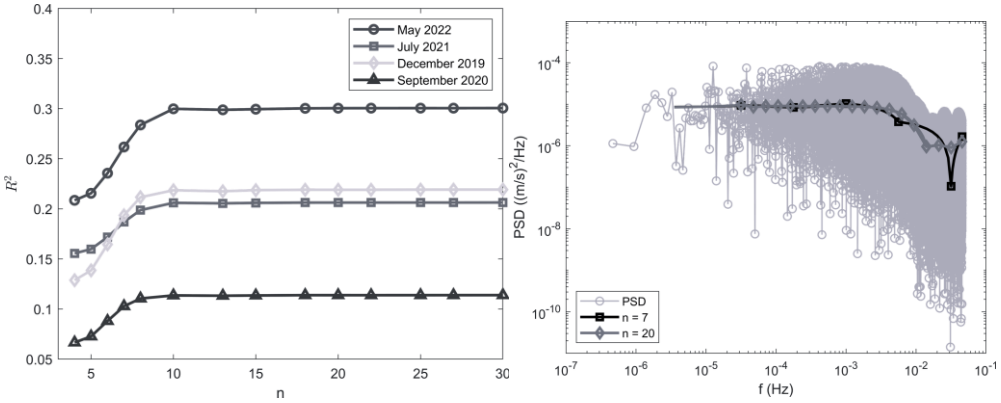

Fig. 12 R^2 vs n for four cases (left) and PSD_a vs frequency (right) for May 2022 varying n

4.2 Analysis of satellite data via "agnostic" approach

This section focuses on the analysis of satellite data via the "agnostic" based approach. Fig. 11 shows how the optimization framework works; specifically, Fig. 11-left depicts how R^2 changes during the convergence process and how many iterations are needed to maximize R^2 in case of n=20 points. Fig. 11-right depicts two different polygonal chain curve, one (labelled A) related to the beginning of the optimization process, and the other (labelled B), related to the end of the optimization process. The results show how the shape of the polygonal chain changes allowing to achieve a best-fit curve at the end of the optimization process.

As already mentioned in Section 0, the "agnostic" approach allows to find the best-fit curve; however, the shape of the best-fit curve depends on the number of points n. To assess the effect of this parameter, several analyses have been carried out varying n from 4 to 30. The results are depicted in Fig. 12; Fig. 12-left shows how R^2 changes varying the number of points n for four different time frames: spring 2022, summer 2021, autumn 2020 and winter 2019. The data highlight that to higher values of n correspond higher values of R^2 in all the examined cases; this result is expected since higher values of n allows to represent more complex shapes of the polygonal chain which can represent, in a more rigorous way, the satellite data. Furthermore, if n is higher than 15 the curve reaches a plateau, this means that further increases of this parameters does not introduce any benefits in terms of increase of R^2. Fig. 12-right shows the shape of the polygonal chains varying the parameter n for the case of spring 2022. Another interesting aspect is related to the value of R^2 obtained by each curve (for n>15). Notably, the spring 2022 dataset yields the highest R^2 value compared to the others. This variability in R^2 is influenced by the level of noise present in the *PSD*, which tends to lower the R^2 values.

To assess if the "agnostic" approach produces a different shape of the *PSD*, hereafter named PSD_a, with respect to the PSD_{vk}, two different cases have been considered, namely winter 2019 and summer 2022, depicted in Fig. 13-left and Fig. 13-right, respectively. In both cases the results show a similar response for low frequency values (up to 10^{-3} Hz) whereas some differences occur at higher frequency values. In addition, the R^2 values are comparable but slightly higher for the PSD_a, indeed, for summer 2022, R^2 is 0.106 for the PSD_{vk} and 0.109 for the PSD_a. Similarly, for winter 2019 the R^2 for the PSD_{vk} is 0.212, while for the agnostic approach is 0.219. This

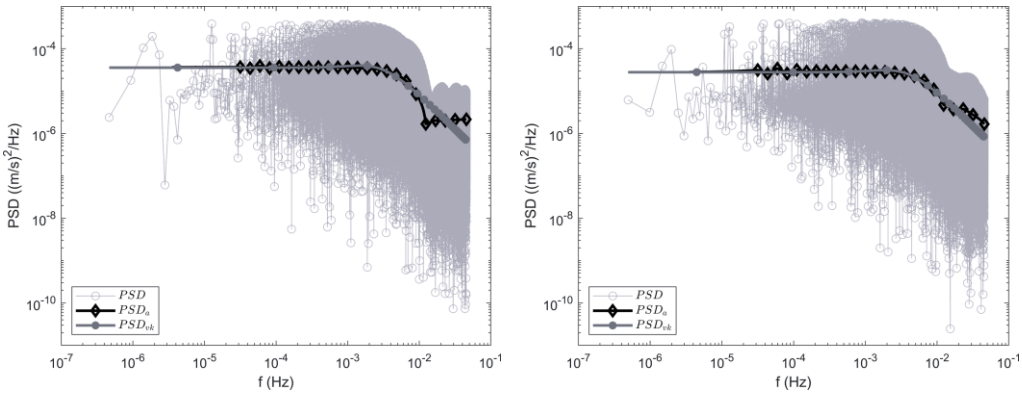

Fig. 13 PSD_a vs PSD_{vk} for winter 2019 (left) and summer 2022 (right)

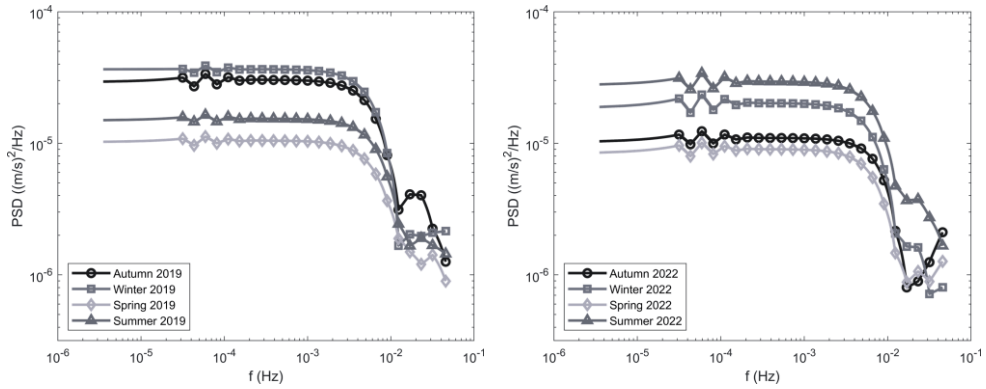

Fig. 14 PSD_{vk} for all seasons of 2019 (left) and 2022 (right)

discrepancy can be attributed to the different behaviour observed at higher frequencies. Indeed, the slope of the best-fit curve is similar for both approaches around 10^{-2} Hz, but it changes for frequency values close to 4×10^{-2} Hz. A variation in the slope of the *PSD* at high frequencies may impact the structural sizing of aeronautical structures, specifically:

- **Dynamic response and vibrational loads:** a steeper *PSD* slope at high frequencies indicates lower energy content at those frequencies, whereas the opposite occurs in case of a flatter slope. A flatter slope affects the response of structural components to high-frequency vibrational loads, as high-frequency vibration modes could be more easily excited, generating localized stresses and material fatigue.
- **Fatigue and cumulative damage:** high frequencies are typically associated with short-term fatigue phenomena and rapid accumulation of microscopic damage. If the *PSD* exhibits a flatter slope (thus more energy), higher-intensity cyclic loading at these frequencies can accelerate fatigue phenomena, particularly in lightweight components, which are typically present in aeronautical structures.
- **Design criteria:** a flatter *PSD* slope at high frequencies implies a potential increase in energy density at those frequencies, necessitating reinforcements or materials with high fracture resistance. Structures exposed to such loads may require specific mitigation measures, such as advanced materials or geometries that reduce sensitivity to crack propagation.

Fig. 14 shows the PSD_a for the year 2019 and 2022.

5. Discussion

The analysis of wing gust spectra via satellite data demonstrates significant potential for detecting and analyzing wind gusts. The proposed approach allows to handle the satellite data in order to monitor wind gust and detect potential changes due to the continuous environmental changes. However, several limitations to this approach must be considered. The Aeolus satellite operates in LEO, which means it does not provide continuous coverage of any single area; therefore, the data related to a specific area are not always available as the satellite only passes over an area twice a day. Consequently, the time signal data must be completed by inserting zeros when the satellite does not cover the region of interest, potentially introducing inaccuracies and increasing noise signal. Even though this aspect represents a drawback, it is at the same time a key point of the LEO satellite, since it allows to cover the entire earth map and to assess *PSD* of different regions all over the world. Indeed, historical data have been gathered via numerous flights along the transatlantic route, whereas LEO satellite can overcome this limitation due to its peculiar characteristics of mapping the entire world. Another drawback is the limited quantity of data which is available since the advent of LEO satellites is recent. This aspect limits the investigation and the assessment of potential effects of climate change on the *PSD* of wind gust since the observation time is limited to a short time window with respect to the typical temporal scales observed in the climate change. Although there are limitations associated with the use of data from LEO satellites, this study demonstrates the integration of the power spectral analysis techniques, commonly used to evaluate the *PSD* of time signals, with satellite-derived data to initialize the discussion regarding a critical question in the structural sizing of aircraft components: is it reasonable, given the ongoing changes in climate, to base the *PSD* of gust loads on data collected nearly a century ago? The authors propose a preliminary methodology leveraging on satellite observations; in this regard the authors acknowledge that it represents only a starting point for more comprehensive and detailed investigations.

Despite these limitations, integrating satellite technology in the analysis of wind gusts represents a significant advancement in aviation safety and efficiency. In the aeronautical context, where reliability and longevity are paramount, understanding *PSD* characteristics is essential for determining component lifespan and developing predictive monitoring and maintenance strategies. Regarding the aircraft design process, the stress level induced by the wind gust is directly proportional to the gust intensity (a vertical gust increases the aircraft angle of attack, so the lift generated by the wings and the bending moment at the root section of the wings). This simple relation can be traduced in the following statement, "*the stronger the gust the higher the stress levels in the wing structural material*", which suggests that new materials with high strength-to-weight ratio property are to be used. In this regard, composite material may be a solution, but it introduces some complexity regarding the manufacturing process. Indeed, when dealing with the manufacturing of composite materials, several defects such as gaps, overlaps, tow kinking and fibre misalignments can occur and jeopardize the actual strength of the final structural component. To deal with this problem, techniques such as Automated Fibre Placement (AFP) and Tow Laying (ATL) are currently investigated (Heinecke *et al.* 2019). Furthermore, the development of computational models which can take into account how the defects can affect the structural components properties are essential (Pagani *et al.* 2021, Pagani *et al.* 2023). Another important

aspect is the long-time effect of several intense gusts on the defects propagations, both in metal and composite material. In fact, potential increase in *PSD* suggests that aeronautical structures may be subjected to greater cyclic stresses, necessitating materials with enhanced fatigue resistance or more frequent maintenance interventions. Multiple high cyclic stress level may promote and facilitate crack propagation, affecting current predictive and maintenance strategies which are to be updated in order to take into account and deal with the potential detrimental effects of climate change. Furthermore, high fatigue resistance materials are to be investigated and novel design tools are to be developed, in the early stage of the aircraft design process, in order to guarantee proper and adequate maintenance strategies which maintain high safety levels. Further development of novel load alleviation techniques are essential in order to deal with high-intensity gust reducing the stress levels of the structural component and the quality of the flight trip of the passengers. The above discussion highlights the potential implications on the aircraft design and maintenance process due to the effects of climate change which can not be neglected in the design of next generation aircraft.

6. Conclusions

Climate change has brought significant challenges to the aviation sector. Among the effects, such as rising temperatures and changes in wind patterns, the increase in wind gust intensity is a major concern highlighted in this paper. The rise in gust intensity poses significant issues for aviation since it may worsen structural fatigue and impacts aircraft performance. In this context, satellite technology can play a crucial role in detecting and analyzing climatic conditions, especially changes in wind gust patterns. This work reveals the potential and capabilities of satellite technology in detecting wind gusts via Aeolus satellite's wind gust data. The power-spectral analysis of wind gust has been used to assess wind gust power spectrum and two different approaches been used: one based on von Kármán model, and the other, named "agnostic", which does not use any pre-defined equation and aims at assessing if potential discrepancies may occur with von Kármán model. Satellite data were used to show seasonal and annual variations in vertical gusts between 2019 and 2022 over an area of the transatlantic route. The analysis demonstrated that variations in some cases between different years and seasons can be detected and lays the foundation to monitor, in the forthcoming years, how the wing gust power spectrum is affected by climate change. A comparison of the two approaches reveals some differences at high-frequency ranges, while no significant discrepancies were observed at lower frequencies. These preliminary findings suggest the possibility to reconsider and potentially update historical gust models in light of ongoing climate changes. Addressing this question is inherently complex; this study aims to lay the groundwork for future analyses that, with access to more comprehensive datasets, could determine whether modifications to the current models are necessary. These aspects are of paramount importance to aircraft manufactures since it will influence the design and maintenance of aircraft designed to enter into service in the next coming years.

Acknowledgments

This study was carried out within the Space It Up project funded by the Italian Space Agency, ASI, and the Ministry of University and Research, MUR, under contract n. 2024-5-E.0 - CUP n.

I53D24000060005.

The Polytechnic of Turin is grateful to the Italian Space Agency for the PhD scholarship ASI - Responsible Space for Sustainability.

References

Abu Salem, K., Palaia, G. and Quarta, A.A. (2023), "Review of hybrid-electric aircraft technologies and designs: Critical analysis and novel solutions", *Progr. Aerosp. Sci.*, **141**, 100924. https://doi.org/10.1016/j.paerosci.2023.100924.

Bagarello, S., Campagna, D. and Benedetti I. (2024), "A survey on hydrogen tanks for sustainable aviation", *Green Energy and Intelligent Transportation*, 100224. https://doi.org/10.1016/j.geits.2024.100224.

Balatti, D., Khodaparast, H.H., Friswell, M.I., Manolesos, M. and Castrichini, A. (2021), "Aircraft turbulence and gust identification using simulated in-flight data", *Aerosp. Sci. Technol.*, **115**, 106805. https://doi.org/10.1016/j.ast.2021.106805.

Crisp, N.H., Roberts, P.C., Livadiotti, S., Oiko, V.T.A., Edmondson, S., Haigh, S.J., ... & Schwalber, A. (2020), "The benefits of very low earth orbit for earth observation missions", *Progr. Aerosp. Sci.*, **117**, 100619. https://doi.org/10.1016/j.paerosci.2020.100619.

De Gaspari, A., Toffol, F., Mantegazza, P. and Mannarino, A. (2016), "Optimal and robust design of a control surface actuation system within the GLAMOUR project", *Aerotec. Missili Spaz*., **95**, 219-231. https://doi.org/10.1007/BF03404730.

ESA, VirES for Aeolus. https://aeolus.services/ (accessed on 19/11/2024).

FAR 25, Gust and turbulence loads. https://www.ecfr.gov/current/title-14/chapter-I/subchapter-C/part-25/subpart-C/subject-group-ECFR3e855ea22ea15d0/section-25.341 (accessed 18/11/2024)

Figueroa, R.Q., Cavallaro, R. and Cini A (2024), "Feasibility studies on regional aircraft retrofitted with hybrid-electric powertrains", *Aerosp. Sci. Technol.*, **151**, 109246. https://doi.org/10.1016/j.ast.2024.109246.

Filippi, M., Tortorelli, E., Petrolo, M. and Carrera, E. (2023), "Refined structural theories for dynamic and fatigue analyses of structure subjected to random excitations", *Mater. Res. Proc.*, **37**, 453-456. https://doi.org/10.21741/9781644902813-100.

Findlay, S.J. and Harrison, N.D (2002), "Why aircraft fail", *Mater. Today*, **5**, 18-25. https://doi.org/10.1016/S1369-7021(02)01138-0.

Flomenhoft, H.I. (2012), "Brief history of gust models for aircraft design", *J. Aircraft*, **31**(5), 1225-1227. https://doi.org/10.2514/3.46637.

Graver, B., Zhang, K. and Rutherford, D (2019), "CO2 emissions from commercial aviation, 2018", *2018 International Council on Clean Transportation.*

Gu, H., Healy, F., Jayatilake, S., Rezgui, D., Lowenberg, M., Cooper, J., ... & Castrichini, A. (2024), "Flight dynamics of aircraft incorporating the semi-aeroelastic hinge", *Aerosp. Sci. Technol.*, **147**, 109026. https://doi.org/10.1016/j.ast.2024.109026.

Gudmundsson, S. (2014), *General Aviation Aircraft Design*, Elsevier.

Hajjem, M., Victor, S., Melchior, P., Lanusse, P. and Thomas, L. (2023), "Wind turbulence modeling for real-time simulation", *Fract. Calc. Appl. Anal*., **26**, 1632-1662. https://doi.org/10.1007/s13540-023-00165-0.

Handojo, V. (2022), "Investigation of load alleviation in aircraft pre-design and its influence on structural mass and fatigue", *Aerosp. Sci. Technol.*, **122**, 107405. https://doi.org/10.1016/j.ast.2022.107405.

He, S., Guo, S., Liu, Y. and Luo W. (2021), "Passive gust alleviation of a flying-wing aircraft by analysis and wind-tunnel test of a scaled model in dynamic similarity", *Aerosp. Sci. Technol.*, **113**, 106689. https://doi.org/10.1016/j.ast.2021.106689.

He, T. and Su, W. (2023), "Robust control of gust-induced vibration of highly flexible aircraft", *Aerosp. Sci. Technol.*, **143**, 108703. https://doi.org/10.1016/j.ast.2023.108703.

Heinecke, F. and Willberg, C. (2019), "Manufacturing-induced imperfections in composite parts manufactured via automated fiber placement", *J. Compos. Sci.*, **56**, 56. https://doi.org/10.3390/jcs3020056.

Hoblit, F.M. (1988), *Gust Loads on Aircraft Concepts*, AIAA Education Series. https://doi.org/10.2514/4.861888.

Jiang, W., Chang, R.C., Yang, N. and Ding, M. (2023), "Movement mechanisms for transport aircraft during severe clear-air turbulence encounter", *Aeronaut. J.*, **127**, 537-561. https://doi.org/10.1017/aer.2022.77.

Jones, A.R. and Cetiner, O. (2021), "Overview of unsteady aerodynamic response of rigid wings in gust encounters", *AIAA J.*, **59**(2), 731-736. https://doi.org/10.2514/1.J059602.

Jones, A.R., Cetiner, O. and Smith, M.J. (2022), "Physics and modeling of large flow disturbances: Discrete gust encounters for modern air vehicles", *Ann. Rev. Fluid Mech.*, **54**(1), 469-493. https://doi.org/10.1146/annurev-fluid-031621-085520.

Jones, R. (2014), "Fatigue crack growth and damage tolerance", *Fatig. Fract. Eng. Mater. Struct.*, **37**, 463-483. https://doi.org/10.1111/ffe.12155.

Kaplan, M.L., Charney, J.J., Waight, K.T., Lux, K.M., Cetola, J.D., Huffman, A.W., ... & Lin, Y.L. (2006), "Characterizing the severe turbulence environments associated with commercial aviation accidents. A real-time turbulence model (RTTM) designed for the operational prediction of hazardous aviation turbulence environments", *Meteorol. Atmos. Phys*., **94**, 235-270. https://doi.org/10.1007/s00703-005-0181-4.

Kharoufah, H., Murray, J., Baxter, G. and Wild, G (2018), "A review of human factors causations in commercial air transport accidents and incidents: From to 2000-2016", *Progr. Aerosp. Sci.*, **99**, 1-13. https://doi.org/10.1016/j.paerosci.2018.03.002.

Lee, J.H., Sevil, H.E., Dogan, A. and Hullender, D. (2013), "Estimation of maneuvering aircraft states and time-varying wind with turbulence", *Aerosp. Sci. Technol.*, **31**, 87-98. https://doi.org/10.1016/j.ast.2013.09.009.

Lee, Y., Kim, S.H., Noh, Y.J. and Kim, J.H. (2023), "Deep learning-based summertime turbulence intensity estimation using satellite observations", *J. Atmosph. Oceanic Technol.*, **40**, 1433-1448. https://doi.org/10.1175/JTECH-D-22-0137.1.

Lomax, T.L. (1996), *Structural Loads Analysis for Commercial Transport Aircraft: Theory and Practice*, American Institute of Aeronautics and Astronautics.

Mehmood, K., Ali Shah, S.I., Ali Shams, T., Mumtaz Qadri, M.N., Khan, T.A. and Kukulka, D. (2023), "Flight dynamic characteristics of wide-body aircraft with wind gust and turbulence", *Fluid.*, **8**(12), 320. https://doi.org/10.3390/fluids8120320.

Morelli, E. and Cunningham, K. (2012), "Aircraft dynamic modeling in turbulence", *AIAA Atmospheric Flight Mechanics Conference*, Minneapolis, Minnesota, August. https://doi.org/10.2514/6.2012-4650.

NASA, Extreme Weather and Climate Change. https://science.nasa.gov/climate-change/extreme-weather/ (accessed 18/11/2024)

Nerushev, A.F., Visheratin, K.N. and Ivangorodsky, R.V. (2022), "Satellite-derived estimations of the clear-air turbulence in the upper troposphere", *IOP Conf. Ser.: Earth Environ. Sci.*, **1040**(1), 012025. https://doi.org/10.1088/1755-1315/1040/1/012025.

Pagani, A. and Sanchez-Majano, A.R. (2021), "Stochastic stress analysis and failure onset of variable angle tow laminates affected by spatial fibre variations", *Compos. Part C: Open Access*, **4**, 100091. https://doi.org/10.1016/j.jcomc.2020.100091.

Pagani, A. and Sanchez-Majano, A.R. (2023), "Analysis of the manufacturing signature on AFP-manufacturesvariable stiffness composite panels", *Mater. Res. Proc.*, **37**, 317-320. https://doi.org/10.21741/9781644902813-69.

Payne, B.W. and Cox, R.A. (1969), "Application of power spectral methods to aircraft gust clearance: A review of the use of power spectral gust design procedures for the computation of design limit loads on civil aircraft", *Aircraft Eng. Aerosp. Technol.*, **41**, 17-24. https://doi.org/10.1108/eb034553.

Press, H. and Bernard, M. (1954), "A study of the application of power-spectral methods of generalized harmonic analysis to gust loads on airplanes", Research Report No. NACA-TN-2853, NASA.

https://ntrs.nasa.gov/citations/19930090975.

Radhakrishnan, C., Chandrasekar, V., Reising, S.C., Berg, W., Brown, S.T., Tanelli, S., ... & Sacco, G.F. (2022), "Cross validation of TEMPEST-D and RainCube observations over precipitation systems", *IEEE J. Selec. Topic. Appl. Earth Observ. Remote Sens.*, **15**, 7826-7838. https://doi.org/10.1109/JSTARS.2022.3199402.

Regan, C.D. and Jutte, C.V. (2012), "Survey of applications of active control technology for gust alleviation and new challenges for lighter-weight aircraft", Research Report No. NASA/TM-2012-216008, NASA. https://ntrs.nasa.gov/citations/20120013450.

Reitebuch, O., Lemmerz, C., Nagel, E., Paffrath, U., Durand, Y., Endemann, M., ... & Chaloupy, M. (2009), "The airborne demonstrator for the direct-detection doppler wind lidar Aladin on Adm-Aeolus. Part I: Instrument design and comparison to satellite instrument", *J. Atmosph. Ocean. Technol.*, **26**, 2501-2515. https://doi.org/10.1175/2009JTECHA1309.1.

Sharman, R. (2016), *Nature of Aviation Turbulence*, Eds. Sharman, R., Lane, T., Springer, Cham.

Storer, L.N., Gill, P.G. and Williams, P.D (2019), "Multi-model ensemble predictions of aviation turbulence", *Meteorolog. Appl.*, **26**, 416-428. https://doi.org/10.1002/met.1772.

Storer, L.N., Williams, P.D., Gill, P.G. (2019), "Aviation turbulence: dynamics, forecasting, and response to climate change", *Pure Appl. Geophys*., **176**, 2081-2095. https://doi.org/10.1007/s00024-018-1822-0.

Tavares, S.M.O. and De Castro, P.M.S.T (2017), "An overview of fatigue in aircraft structures", *Fatig. Fract. Eng. Mater. Struct.*, **40**, 1510-1529. https://doi.org/10.1111/ffe.12631.

Toffol, F. and Ricci, S. (2023), "Development of an active wingtip for aeroelastic control", *Aerosp.*, **10**(8), 693. https://doi.org/10.3390/aerospace10080693.

Wangì, K., Yu, Y., Gong, Y., Yi, Y. and Zhang, X. (2023), "On-earth observation of low earth orbit targets through phase disturbances by atmospheric turbulence", *Remote Sens.*, **15**(19), 4718. https://doi.org/10.3390/rs15194718.

Witschas, B., Lemmerz, C., Geiß, A., Lux, O., Marksteiner, U., Rahm, S., ... & Weiler, F. (2020), "First validation of Aeolus wind observations by airborne Doppler wind lidar measurements", *Atmosph. Measure. Techniq.*, **13**, 2381-2396. https://doi.org/10.5194/amt-13-2381-2020.

Wu, Z., Cao, Y. and Ismail, M (2019), "Gust loads on aircraft", *Aeronaut. J.*, **123**, 1216-1274. https://doi.org/10.1017/aer.2019.48.

Yuan, W., Zhang, X., Poirel, D. and Wall A. (2024), "Numerical modelling of aerodynamic response to gusts and gust effect mitigation", *Aerosp. Sci. Technol.*, **154**, 109467. https://doi.org/10.1016/j.ast.2024.109467.

CC

Appendix A

Table 1 contains data on the von Kármán model parameters described in Section 0. The aircraft speed V is equal to 236 m/s.

Table 1 Data of the von Kármán model parameters described in Section 0

Month	Year	R^2	L [m]	σ [m/s]
May	2019	0.252	13072	9.10×10^{-4}
	2020	0.137	13182	8.54×10^{-4}
	2021	0.138	13163	8.99×10^{-4}
	2022	0.175	13157	8.79×10^{-4}
July	2019	0.211	12442	1.05×10^{-3}
	2020	0.161	10494	1.24×10^{-3}
	2021	0.193	10832	1.21×10^{-3}
	2022	0.107	9123	1.50×10^{-3}
September	2019	0.106	10241	1.43×10^{-3}
	2020	0.110	11979	1.70×10^{-3}
	2021	0.081	10026	1.50×10^{-3}
	2022	0.192	12791	9.45×10^{-4}
December	2019	0.212	11745	1.50×10^{-3}
	2020	0.100	7072	1.90×10^{-3}
	2021	0.166	9988	1.52×10^{-3}
	2022	0.240	12179	1.15×10^{-3}